Electronic bonding transition in compressed SiO_2 glass

Jung-Fu Lin,[1] Hiroshi Fukui,[2] David Prendergast,[3,4] Takuo Okuchi,[5] Yong Q. Cai,[6] Nozomu Hiraoka,[6] Choong-Shik Yoo,[1] Andrea Trave,[1] Peter Eng,[7] Michael Y. Hu,[8] and Paul Chow[8]

[1]*Lawrence Livermore National Laboratory, 7000 East Avenue, Livermore, California 94550, USA*

[2]*Institute for Study of the Earth's Interior, Okayama University, Yamada 827, Misasa, Tottori 682-0193, Japan*

[3]*Department of Physics, University of California at Berkeley, Berkeley, California 94720, USA*

[4]*Chemical Sciences Division, Lawrence Berkeley National Laboratory, Berkeley, California 94720, USA*

[5]*Institute for Advanced Research, Nagoya University, Furo-cho, Chikusa, Nagoya 464-8601, Japan*

[6]*National Synchrotron Radiation Research Center, Hsinchu 30076, Taiwan*

[7]*Consortium for Advanced Radiation Sources, The University of Chicago, Chicago, Illinois 60637, USA*

[8]*HPCAT, Carnegie Institution of Washington, Advanced Photon Source, Argonne National Laboratory, 9700 South Cass Avenue, Argonne, Illinois 60439, USA*

(Received 7 September 2006; published 5 January 2007)

Knowledge of the electronic structure of amorphous and liquid silica at high pressures is essential to understanding their complex properties ranging from silica melt in magma to silica glass in optics, electronics, and material science. Here we present oxygen near *K*-edge spectra of SiO_2 glass to 51 GPa obtained using x-ray Raman scattering in a diamond-anvil cell. The x-ray Raman spectra below ~10 GPa are consistent with those of quartz and coesite, whereas the spectra above ~22 GPa are similar to that of stishovite. This pressure-induced spectral change indicates an electronic bonding transition occurring from a fourfold quartzlike to a sixfold stishovitelike configuration in SiO_2 glass between 10 GPa and 22 GPa. In contrast to the irreversible densification, the electronic bonding transition is reversible upon decompression. The observed reversible bonding transition and irreversible densification call for a coherent understanding of the transformation mechanism in compressed SiO_2 glass.

DOI: 10.1103/PhysRevB.75.012201 PACS number(s): 64.70.Pf, 61.10.Ht, 61.43.Fs, 64.60.−i

Silicon dioxide (SiO_2) exists in a wide-range of polymorphs in nature including α-quartz, coesite, stishovite, and disordered silica. Crystal structures of these polymorphs consist mainly of edge- and corner-sharing tetrahedra and octahedra, which are also the most fundamental building blocks of three-dimensional framework structures commonly found in minerals and synthetic materials.[1–12] The thermal, optical, electronic, and mechanical properties of SiO_2 polymorphs vary greatly depending on subtle differences in the long- and short-range order, the electronic bonding, the degree of ionicity, and the coordination number.[6–10,12] Therefore, there have been numerous investigations to determine various physical properties of SiO_2 in crystalline, amorphous, and liquid states at high pressures and temperatures.[1–12]

The pressure-induced structural phase transitions of crystalline SiO_2 phases have been well studied in the context of increasing coordination number in silicon; from four in α-quartz and coesite to six in stishovite, to eight in a pyrite phase recently discovered.[13] On the other hand, the exact nature of the pressure-induced change in amorphous SiO_2 has been unsettled.[1,4,5] For example, previous infrared[4] and x-ray diffraction[5] studies suggested that a continuous transformation from the four- to sixfold coordinated silicon occurred in amorphous SiO_2 at high pressures, whereas separate Raman studies attributed to a pressure-induced shift in the local ring statistics and a breakdown in the intermediate-range order.[1] This discrepancy arises from the fact that these optical spectra cannot be uniquely assigned without knowing the structure of the silica glass.

Electron-energy loss near-edge spectroscopy (ELNES) and x-ray absorption near-edge spectroscopy (XANES) have been successful in probing the electronic bonding in both amorphous and crystalline SiO_2 at ambient conditions.[14–17] However, because of the relatively low-energy electronic states of oxygen (i.e., 520 eV to 580 eV for the *K* edge) and/or the multiple electron scattering effect in high-energy ELNES, the applications of these techniques are limited to surface structures in a high-vacuum environment, not applicable to high-pressure samples. Knowledge on the change of the electronic bonding in the compressed SiO_2 glass is often limited to the studies on the quenched samples.[2] Here we have employed an inelastic x-ray Raman scattering (XRS) method to probe the oxygen *K*-edge absorption spectra and the electronic bonding in SiO_2 glass in a diamond anvil cell (DAC).[18–21] Comparing with previous ELNES spectra,[14–17] our present XRS studies and theoretical calculations indicate that SiO_2 glass undergoes a reversible electronic bonding transition from a fourfold quartzlike to a sixfold stishovitelike configuration between 10 GPa and 22 GPa.

The oxygen near *K*-edge XRS experiments of compressed SiO_2 glass were conducted on the 16-IDD sector of the HP-CAT and the 13-IDD sector of the GSECARS, APS,[18–20] and the Taiwan Beamline BL12XU at SPring-8 (Ref. 21). A beryllium gasket, transparent to the incoming and outgoing x-ray, of 3 mm in diameter was preindented by a pair of diamonds having culets 500 μm across to a thickness of 50 μm and a hole of 250 μm in diameter was drilled in it and used as the sample chamber. SiO_2 glass (99.9% pure) was loaded into the sample chamber of a DAC with a few ruby spheres as the pressure calibrant. The XRS spectra were collected using the reverse scan technique: the inelastically scattered x-ray Raman signals were collected at an angle (2θ) of 30° with an array of spherical Si analyzers and a Si

detector in near backscattering geometry at a fixed energy of 9.886 keV at BL12XU and 9.686 keV (E_0) at GSECARS and HPCAT, while the incident monochromatic x-ray beam (E) from a Si(111) or C(111) double crystal monochromator was scanned over the energy range of E-E_0 from 520 eV to 575 eV. The total energy resolution was ~1.1 eV. The incident x-ray beam was focused onto the sample with a beam size of 80 μm horizontally and 20 μm vertically. The counting time for each XRS spectrum was approximately 1 h, and 10–20 spectra were collected and added at each pressure to obtain a reasonably good statistics. The pressure uncertainty (1σ) was estimated to be 3–5%, based on the multiple pressure measurements from the ruby spheres in the sample chamber.

For direct comparison with the XRS spectra of compressed SiO_2 glass, XRS spectra of polycrystalline α-quartz, coesite,[22] and stishovite were also collected on the BL12XU sector at SPring-8 under ambient conditions.[21] The crystal structures of the materials were confirmed by x-ray diffraction and Raman spectroscopy before and after the experiments. The XRS spectra for α-quartz and stishovite were collected with an energy resolution of ~250 meV at a scattering angle of 40°, whereas the XRS spectrum for coesite was collected with an energy resolution of ~1.1 eV at a scattering angle of 30°. The high-energy resolution of ~250 meV was achieved by the use of an additional Si(400) high-resolution monochromator, and the inelastically scattered x-ray was collected by a Si(555) analyzer mounted on the two-meter spectrometer.[21]

Figure 1 summarizes the pressure-induced changes of the oxygen near K-edge XRS spectra in SiO_2 glass to 51 GPa at 300 K. The most characteristic feature of the XRS spectra below 14 GPa is an intense peak located at ~538 eV, which is attributed to the electronic transition of oxygen 1s to 2p states hybridized with the silicon 3s and 3p states in the tetrahedrally coordinated SiO_2 such as that in α-quartz and coesite (Figs. 1 and 2).[14–17] While no prominent change in the XRS spectra is observed at pressures below 14 GPa, a broad, intense peak, centered at ~544 eV, occurs between 26 GPa and 51 GPa, which resembles the bonding feature of the octahedrally coordinated stishovite (Fig. 2).[16,17]

Using first principles, density functional theory calculations, we have verified the spectroscopic differences between α-quartz and stishovite using a plane-wave pseudopotential approach already applied successfully to describing the x-ray absorption cross section of ice and water[23] [Fig. 2(c)]. We modeled the x-ray excitation using a core-hole pseudopotential and the associated excited electron introduced as impurities in a large supercell of the crystal under periodic boundary conditions. We used a supercell of 243 and 216 atoms and expanded the electronic wave functions using a kinetic energy cutoff of 80 and 120 Ry for quartz and stishovite, respectively. Our spectra have been calculated using a converged Brillouin zone sampling of up to 64 k points for these large supercells. Rather than using the local density approximation and computing a prohibitive number of unoccupied bands employed in previous studies using localized basis sets,[24] we used the Perdew-Burke-Ernzerhof generalized-gradient exchange-correlation functional[25] together with the recursion method to directly generate the x-ray absorption cross section.[26]

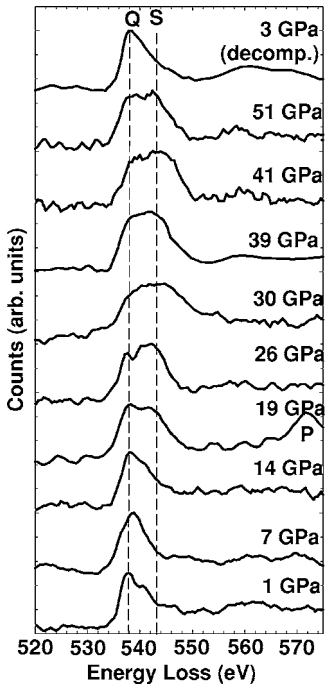

FIG. 1. Oxygen K-edge spectra in compressed SiO_2 glass by x-ray Raman spectroscopy. The main feature of the spectra between 1 GPa and 14 GPa is an intense peak located at ~538 eV (labeled as Q), whereas an additional, intense peak appears at ~544 eV at pressures above 19 GPa (labeled as S). The spectrum at 3 GPa was collected from the sample quenched from ~45 GPa. No prominent post edge feature above 547 eV is observed because of the low statistics resulting from the XRS experiments in a high-pressure DAC. P, an unidentified peak at 10.459 keV (likely due to micro x-ray diffraction); the peak intensity changed significantly when the taken-off angle (2θ of ~30°) was varied.

The electronic structure of silica probed near the oxygen K edge is sensitive to the local environment of the excited oxygen atom. In stishovite at 40 GPa, our calculations verify that each oxygen atom has three nearest-neighbor silicon atoms at a distance of 1.72 Å, one nearest-neighbor oxygen at a distance of 2.24 Å bonded to two of these silicons, and eight more oxygens slightly farther away at 2.44 Å. Examination of the partial electronic density of states indicates strong oxygen p and silicon s hybridization at ~538 eV and p-p hybridization with nearby oxygens at both ~538 eV and ~544 eV, leading to the two oxygen near K-edge peaks which differentiate bonding character of stishovite from α-quartz.

Based on our XRS spectra and calculations, previous multiple-scattering calculations and ELNES and XANES spectra in crystalline and amorphous SiO_2 under ambient conditions,[14–17] it is known that the oxygen near K-edge spectra are sensitive to the change of the coordination number in SiO_2 but variations in the bond length and bonding angles only have a minor influence on the spectra, as evident from the XRS features of α-quartz, coesite, and stishovite shown in Fig. 2. For example, α-quartz and coesite have nearly identical XRS features and consist of the same SiO_4

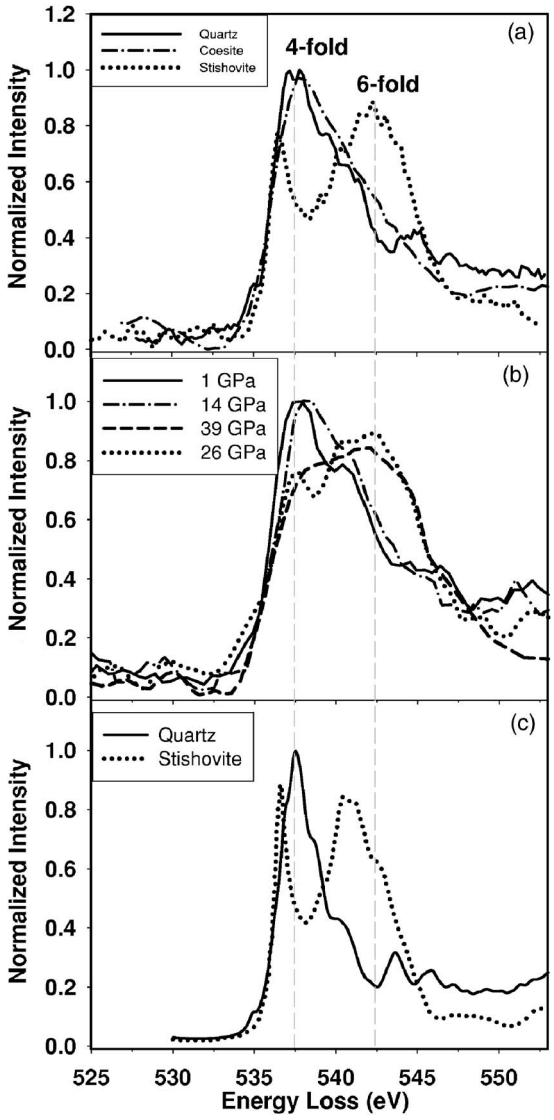

FIG. 2. Oxygen *K*-edge spectra in SiO_2 crystals (a) and glass (b) by x-ray Raman spectroscopy. These spectra were normalized by the integrated intensity from energy range between 534 eV and 547 eV. The intense peak at ~538 eV in α-quartz and coesite arises from the tetrahedral bonding, whereas the most intense peak at ~544 eV in stishovite is attributed to the octahedral bonding (Refs. 14–17). (c) First principles, theoretically calculated oxygen *K*-edge spectra for α-quartz at 0 GPa and stishovite at 40 GPa.

tetrahedron with subtle differences in the Si-O bond distances, the Si-O-Si bond angles, and the total number of tetrahedra engaged in the rings. On the other hand, the XRS spectrum of the octahedrally coordinated stishovite differs significantly from that of α-quartz and coesite due to the change of the coordination number.

The intense peak, centered at ~544 eV, originates from the electron excitation in SiO_6 octahedra in SiO_2 glass, and its appearance indicates an electronic bonding transition from the fourfold quartzlike to the sixfold stishovitelike electronic configuration in compressed SiO_2 glass (Figs. 1 and 2). Nevertheless, this peak centered at 544 eV is substantially broader than the corresponding peak in stishovite. Such a peak broadening could not be simply explained by the

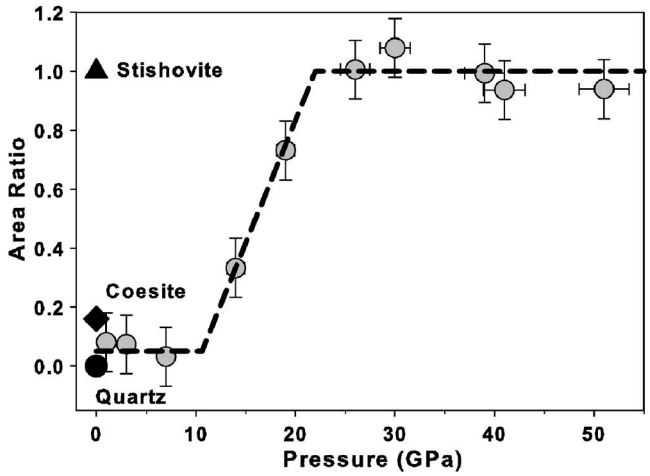

FIG. 3. Normalized and integrated peak intensity of the sixfold stishovitelike bonding as a function of pressure (gray circles). The XRS spectra between 534 eV and 547 eV were first normalized to 1, and the peak region resembling the octahedral bonding from 540 eV to 547 eV were then integrated after subtracting the spectrum from that of α-quartz (solid circle) collected at ambient conditions and setting the fraction of the integrated area ratio of stishovite (solid triangle) to one. The integrated area ratio of coesite (solid diamond) is also plotted for comparison. The dashed line is a guide to the change of the integrated area ratio as a function of pressure.

pressure gradients in the sample chamber. Although the relatively low-energy resolution of ~1.1 eV used to obtain the high-pressure spectra (instead of 250 meV for the stishovite spectrum at the ambient pressure) can be attributed to part of the peak broadening, the possible presence of the fivefold coordination defects should also broaden the peaks due to their irregular geometry and hybridization between neighboring atoms. Further studies are needed to understand the spectral and bonding characteristics of potential fivefold coordination defects in SiO_2 glass,[27,28] which would help understand their contribution to the peak broadening and evaluate further details of the present XRS spectra.

To quantify the electronic bonding transition in compressed SiO_2 glass, we have analyzed the oxygen *K*-edge XRS spectra between 534 eV to 547 eV and obtained the relative abundance of the stishovitelike bonding in SiO_2 glass as a function of pressure (Fig. 3). This procedure has been successfully used to identify the abundance of π^* and σ^* bonds in compressed borate.[19] As shown in Fig. 3, the integrated area ratio between 540 eV and 547 eV significantly increases above ~10 GPa and flattens at above ~22 GPa, indicating a substantial change in the electronic bonding from the quartzlike to the stishovitelike configuration between 10 GPa and 22 GPa. The observed transition range is consistent with previous infrared measurements,[4] but is much narrower than that suggested by previous x-ray diffraction study.[5] The XRS spectrum at 3 GPa, collected upon decompression after the sample was compressed to ~45 GPa, is similar to that of the starting SiO_2 glass and α-quartz. This clearly indicates that the electronic bonding transition occurs reversibly in SiO_2 glass, which is in contrast to the irreversible densification in pressure-quenched silica. A progressive decrease in the mean Si-O-Si angle in

the SiO_4 tetrahedra, which leads to the gradual, continuous densification and rearrangements of oxygen atoms in compressed silica glass,[2] is believed to be responsible for the irreversible densification of SiO_2 glass previously observed at high pressures.[1,14]

Our XRS studies provide conclusive evidence for a fourfold, quartzlike to a sixfold, stishovitelike electronic bonding transition in compressed silica glass. A similar transformation is expected to occur in silicate glasses and melts,[4,11] amorphous GeO_2 (Ref. 10), and amorphous CO_2 (Ref. 29) under pressures, which will most definitely alter their physical, mechanical, and transport properties. Therefore, our present results may have important geophysical implications, considering SiO_2 and $MgSiO_3$ are two major components of magma in the Earth's deep interior. Silicon coordinated with five oxygen atoms has been observed in high-temperature quenched silicates[27] and predicted theoretically,[28,30] and its potential presence in compressed silica glass and liquid could be of key importance in the mechanism in which viscous flow takes place deep in the magma chamber.[30] Although our observed electronic bonding transition in silica glass is reversible upon decompression at room temperature, high temperature should affect the reversibility of the transformation because sixfold coordinated silicon has been detected in quenched silicates and silica.[2,28] Future studies on the high-temperature effect should help gain more insight of the predicted electronic bonding transition in the compressed SiO_2 and $MgSiO_3$ melts deep inside the Earth.[11,30] Should such an electronic transition occur in the silica glass used for high-power laser optics[9] and electronics,[7] there will be significant changes in the optical, mechanical, and electronic properties across the transition, limiting the use of the silica glass at such high-pressure-temperature conditions.

We acknowledge HPCAT and GSECARS, APS, ANL and BL12XU, SPring-8 and NSRRC for the use of the synchrotron facilities. We thank I. Jarrige, H. Ishii, N. Ito, and S. Ghose for their assistance in the high-pressure XRS experiments and J. R. Smyth and S. D. Jacobsen for the coesite sample. We are indebted to E. Schwegler and M. Newville for helpful discussions. The work performed at BL12XU was partly supported by the NSC of Taiwan. This work and use of the APS are supported by U.S. DOE, Basic Energy Sciences, Office of Science, under Contract No. W-31-109-ENG-38, and the State of Illinois under HECA. This work at LLNL was performed under the auspices of the U.S. DOE by UC/LLNL under Contract No. W-7405-Eng-48. H.F. is supported by the 21st century COE program of ISEI. D.P. is supported by NSF Grant No. DMR04-39768 and by the U.S. DOE under Contract No. DE-AC02-05CH11231.

[1] R. J. Hemley, H. K. Mao, P. M. Bell, and B. O. Mysen, Phys. Rev. Lett. **57**, 747 (1986).
[2] E. M. Stolper and T. J. Ahrens, Geophys. Res. Lett. **14**, 1231 (1987).
[3] R. J. Hemley, A. P. Jephcoat, H. K. Mao, L. C. Ming, and M. H. Manghnani, Nature **334**, 52 (1988).
[4] Q. Williams and R. Jeanloz, Science **239**, 902 (1988).
[5] C. Meade, R. J. Hemley, and H. K. Mao, Phys. Rev. Lett. **69**, 1387 (1992).
[6] D. J. Lacks, Phys. Rev. Lett. **80**, 5385 (1998).
[7] D. A. Muller, T. Sorsch, S. Moccio, F. H. Baumann, K. Evans-Lutterodt, and G. Timp, Nature **399**, 758 (1999).
[8] A. Trave, P. Tangney, S. Scandolo, A. Pasquarello, and R. Car, Phys. Rev. Lett. **89**, 245504 (2002).
[9] A. Salleo, S. T. Taylor, M. C. Martin, W. R. Panero, R. Jeanloz, T. Sands, and F. Y. Genin, Nat. Mater. **2**, 796 (2003).
[10] M. Guthrie, C. A. Tulk, C. J. Benmore, J. Xu, J. L. Yarger, D. D. Klug, J. S. Tse, H-k. Mao, and R. J. Hemley, Phys. Rev. Lett. **93**, 115502 (2004).
[11] L. Stixrude and B. Karki, Science **310**, 297 (2005).
[12] R. Martonak, D. Donadioi, A. R. Oganov, and M. Parrinello, Nat. Mater. **5**, 623 (2006).
[13] Y. Kuwayama, K. Hirose, N. Sata, and Y. Ohishi, Science **309**, 923 (2005).
[14] I. Davoli, E. Paris, S. Stizza, M. Benfatto, M. Fanfoni, A. Gargano, A. Bianconi, and F. Seifert, Phys. Chem. Miner. **19**, 171 (1992).
[15] D. Li, G. M. Bancroft, M. Kasrai, M. E. Fleet, R. A. Secco, X. H. Feng, K. H. Tan, and B. X. Yang, Am. Mineral. **79**, 622 (1994).
[16] T. Sharp, Z. Wu, F. Seifert, B. Poe, M. Doerr, and E. Paris, Phys. Chem. Miner. **23**, 17 (1996).
[17] Z. Wu, F. Jollet, and F. Seifert, J. Phys.: Condens. Matter **10**, 8083 (1996).
[18] W. L. Mao, H.-K. Mao, P. J. Eng, T. P. Trainor, M. Newville, C.-C. Kao, D. L. Heinz, J. F. Shu, Y. Meng, and R. J. Hemley, Science **302**, 425 (2003).
[19] S. K. Lee, P. J. Eng, H.-K. Mao, Y. Meng, M. Newville, M. Y. Hu, and J. F. Shu, Nat. Mater. **4**, 851 (2004).
[20] Y. Meng, H.-K. Mao, P. J. Eng, T. P. Trainor, M. Newville, M. Y. Hu, C.-C. Kao, J. F. Shu, D. Hausermann, and R. J. Hemley, Nat. Mater. **3**, 111 (2004).
[21] Y. Q. Cai, H.-K. Mao, P. C. Chow, J. S. Tse, Y. Ma, S. Patchkovskii, J. F. Shu, V. Struzhkin, R. J. Hemley, H. Ishii, C. C. Chen, I. Jarrige, C. T. Chen, S. R. Shieh, E. P. Huang, and C. C. Kao, Phys. Rev. Lett. **94**, 025502 (2005).
[22] J. R. Smyth and C. J. Hatton, Earth Planet. Sci. Lett. **34**, 284 (1977).
[23] D. Prendergast and G. Galli, Phys. Rev. Lett. **96**, 215502 (2006).
[24] S. D. Mo and W. Y. Ching, Appl. Phys. Lett. **78**, 3809 (2001).
[25] J. P. Perdew, K. Burke, and M. Ernzerhof, Phys. Rev. Lett. **77**, 3865 (1996).
[26] M. Taillefumier, D. Cabaret, A. M. Flank, and F. Mauri, Phys. Rev. B **66**, 195107 (2002).
[27] J. F. Stebbins, Nature **351**, 638 (1991).
[28] J. R. Rustad, D. A. Yuen, and F. J. Spera, Chem. Geol. **96**, 421 (1992).
[29] M. Santoro, F. A. Gorelli, R. Bini, G. Ruocco, S. Scandolo, and W. A. Crichton, Nature **441**, 857 (2006).
[30] J. D. Kubicki, R. J. Hemley, and A. M. Hofmeister, Am. Mineral. **73**, 941 (1988).